Title: Targets of sexual selection on the *Drosophila* wing

Authors: Stephen P. De Lisle*, Anneli Brändén, Ellen Pääjärvi Våg

Department of Environmental and Life Science
Karlstad University
Universitetsgatan 2 65188
Karlstad, Sweden

*Corresponding author. Email: stephen.de.lisle@kau.se

Data Availability: Data and code are available at https://doi.org/10.5281/zenodo.13358353

Author Contributions: All authors contributed to data collection and processing. SPD analyzed the data and wrote the paper

Acknowledgements. We thank Jessica Abbott for comments on the manuscript, and John Stinchcombe, Masahito Tsuboi, Miguel Gomez and Erik Svensson for discussion of the methods and results.

Funding: Funding was provided by grants from the Swedish Research Council (VR 2019-03706), Craaford Foundation (20220602), and Royal Physiographical Society of Lund to S.P.D.

Conflict of Interest: The authors have no conflict of interest to declare.

Title: Targets of sexual selection on the *Drosophila* wing

Abstract. Identification of traits causally linked to fitness allows for direct tests of the adaptive value of traits. In the case of *Drosophila* and other insects, wing interference patterns – striking structural color variation generated by optical thin-film interference – have been implicated in mate choice and sexual selection. Yet, we expect wing interference patterns may covary with many aspects of wing morphology, such as size and shape. Here, we used a competitive mating assay in *Drosophila melanogaster* to assess the degree to which sexual selection acts on wing color independently of wing size and shape. We found that 16% of multivariate wing color, and 17% of corresponding estimated wing thickness, can be explained by wing size and shape. Selection analysis revealed that sexual selection on the multivariate combination of color traits most strongly correlated with fitness, as identified by a projection pursuit regression using only color traits, was only apparent; selection on this color axis was eliminated when including multivariate shape. However, significant selection on other combinations of color traits remains even after accounting for wing morphology. Our results suggest that sexual selection may act on a complex combination of wing color and morphology in flies.

Keywords: Sexual selection, geometric morphometrics, phenotypic selection, wing interference patterns

Introduction

Elaborate display traits are commonplace in nature and are often a clear outcome of sexual selection. In most cases, mating display traits are some of the most striking features of the organisms that express them, and as such their existence and importance long noted by naturalists (1-4). An intriguing exception to this lies in the Diptera, where striking wing coloration patterns have only been identified relatively recently as a potential mating display trait (5, 6). Wing interference patterns are bold, iridescent color patterns clearly visible on otherwise-transparent fly wings under certain lighting conditions (Figure 1). These color patterns are formed by the phenomenon of optical thin-film interference, the same physical process that generates iridescent colors on soap bubbles and oil films (6). These colors are formed by interference between light waves reflected off of the top surface of the wing and light waves that travel through the wing to be reflected off of the back surface; the combination of wing thickness and refractive index determines difference in speed between the two light waves and the resulting interference color generated (7). Thus, wing interference patterns are the result of two structural features of fly wings; wing thickness and refractive index, the latter of which is expected to be relatively constant.

Recent work has highlighted wing interference patterns as a potential key trait in sexual selection and species divergence in flying insects. Diptera and other insect species are readily distinguished taxonomically on their wing interference patterns, which are often sexually dimorphic (6, 8-11). In fruit flies, *Drosophila,* wing interference patterns have been shown to be under sexual selection in males (5), and wing interference patterns evolve in response to experimental manipulation of sexual selection (12). Consistent with the latter result, wing interference patterns are also observed to be heritable in different lineages of *D. melanogaster* (5, 13), and wings are known to be important for courtship in *Drosophila* (14).

50 All of the above evidence suggests that wing interference patterns are an important target of
51 sexual selection in flies, and particularly in *D. melanogaster*.
52 Unlike some other elaborate display traits, wing interference colors are inevitably
53 produced by transparent thin films, and thus are expected to be associated with such
54 structures even if not a target of selection themselves. For example, in their comparative
55 study of hoverflies, Li et al. (2023) found a strong relationship between wing size and
56 interference reflectance spectra (and inferred wing thickness). Of past studies of *Drosophila*,
57 only Li (13) included some measure of wing morphology (wing length and width). Thus it is
58 unclear the extent to which wing interference color is related to wing shape in *Drosophila,*
59 which is noteworthy given the pervasive variation in wing shape maintained over deep time
60 (15, 16), and that wing size and shape differ across the sexes (17). Here, we combine a mate
61 choice assay in *Drosophila melanogaster* with detailed measurements of male wing
62 interference color and multivariate wing morphology, in order to perform multivariate
63 selection analysis (18, 19) and identify the targets of sexual selection on the *Drosophila*
64 wing. Our results indicate that while wing color is a direct target of sexual selection,
65 selection appears to act on a complex combination of wing interference color, size, and
66 shape.
67
68 **Methods**
69 *Data collection*
70 Each wild type male fly (LH_m background) was placed in a vial with two other unmated flies,
71 a male and a female each homozygous for the *bw* brown eyed mutation but otherwise of
72 similar genetic background. After 24 hours all flies were removed, resulting offspring
73 allowed to develop, counted and scored for eye color; flies with wild type (red) eyes were
74 sired by the focal male, giving a measure of binomially-distributed reproductive success in a

75 competitive mating context, and thus a relevant component fitness measure for measuring
76 sexual selection (20). This is a standard approach for assessing competitive mating success in
77 *Drosophila* (21); further details on the flies in this study can be found in (22). We focused
78 on the binomial measure of absolute fitness (red-eyed offspring : brown-eyed offspring) in
79 subsequent phenotypic selection analysis; this is appropriate because mate choice occurred
80 within vials, and so relativizing across the entire set of vials would be inappropriate (23).
81 Following this assay, all flies were frozen, thawed and left at room temperature. The right
82 wing of each focal fly was then removed and photographed under a stereomicroscope
83 (Olympus SZX-16) fitted with a 0.8x plan-apochromatic objective; the objective was aligned
84 with the photographic optical path to minimize distortion and chromatic aberration. In case
85 of excessive damage to the right wing, the left wing was instead photographed and the
86 resulting image inverted digitally on the horizontal axis. Wings were placed under a cover
87 slip on a microscope slide placed over an open aperture, and illuminated from above with a
88 ring light to reveal interference patterns (see Figure 1). White balance on the camera (Nikon
89 D850) was customized for the ring light illuminator, and all images were taken at identical
90 exposure, illumination settings, and magnification. Otherwise-unmanipulated raw image
91 files were downsized to 2000 x 3000 pixels for ease of analysis (noting that the native
92 resolution of the camera exceeds the resolving power of the optical system) and saved as
93 RGB jpeg files.
94 For each wing image, we placed 12 fixed landmarks by hand on vein intersections,
95 using the same 12 landmarks that have been widely used to characterize variation in
96 *Drosophila* wing shape (15, 16). We then performed a Procrustes rotation and scaling of
97 these landmarks, followed by principle component analysis of the resulting geometric
98 morphometric data to obtain 20 principle components describing multivariate wing shape.
99 We retained all 20 components in subsequent analysis, as extensive past work in *D.*

100 *melanogaster* suggests that all components harbor genetic variance (15). We also retained
101 centroid size as a measure of overall wing size. We performed landmark placement,
102 Procrustes analysis, and the principle component analysis using the *geomorph* package in R
103 (24).

104 We obtained information on wing interference color by using the color histogram tool
105 in Fiji (25) to calculate mean values for red, green, and blue color channels for manual
106 selections of regions of each wing. Although other studies have focused instead on the color
107 triplet of hue, saturation, and brightness, we focus on RGB color because this is the data
108 recorded by a camera sensor. We focused on four major wing panels that are clearly
109 demarcated by vein intersections and capture most of the wing surface area (Figure 1A),
110 resulting in a total of 12 color traits for each wing. We rotated this data in a PCA to obtain 12
111 orthogonal color variables. We also calculated mean RGB values for the entire manually-
112 selected wing, and present analysis of this simplified color data alongside our analysis of the
113 12 dimensional color data.

114 We used an inverse colorimetry approach to infer the average thickness of each of the
115 four wing panels for each fly. In our images, thin film interference generates reflectance
116 spectra that are recorded by a Bayer sensor in the digital camera. A direct estimate of the
117 reflectance spectra (e.g., 10) would allow direct calculation of thickness of a film with known
118 refractive index. In our case, however, our recordings of the spectra were not direct; rather,
119 the camera records light intensities in three color channels (26). While there are multiple
120 reflectance spectra that could generate any given RGB triplet, it is possible to generate a
121 "most likely" estimated reflectance spectrum by taking the centroid of all possible spectra
122 that could generate a given RGB triplet (27, 28). We performed such an analysis using the
123 invert() function in the coloSpec package in R (27). We inferred spectra from the mean RGB
124 value for separately each wing panel, over a wavelength range of 450-650 nanometers

125 (corresponding to the peak transmittance range of the UV-IR cutoff filter of most digital
126 camera sensors), and assuming a color temperature of 5600K corresponding to the Schott
127 ring light illumination used. Inferred reflectance spectra are illustrated in Figure S1. We
128 then used nonlinear least squares to fit equation 8 from
129 (https://farbeinf.de/pdf/soapfilmcalc.pdf) to each inferred reflectance spectrum, estimating
130 two parameters: a constant, C, and s, where s is parameter that is related to the product of
131 wing thickness (d) and refractive index of the wing (n) by $s = 2dn$. We were then able to
132 calculate wing thickness in nanometers assuming a refractive index of chitin of $n = 1.53$. All
133 nonlinear models converged and yielded estimated thickness values in the expected order of
134 magnitude (approximately several hundred nanometers), however we emphasize that our
135 inferences of wing thickness should be viewed with extreme caution; without spectrometer
136 measures, we present them primarily as a proof of concept. We excluded several outliers
137 from downstream analysis as they had extreme leverage in regressions with fitness.
138
139 *Data analysis*
140 For each male fly we thus obtained data on reproductive success, multivariate wing
141 morphology (20 shape PCs plus centroid size) and multivariate wing interference color (12
142 color PCs). Although we perform a full linear selection analysis with all 33 traits as
143 predictors of fitness, our main aim was to understand how wing interference color is related
144 to wing size and shape, and how any such relations may impact our inference of sexual
145 selection on wing color. Given the highly multivariate nature of the data and our specific
146 aims, we took the following approach to data analysis.
147 First, we used redundancy analysis (RDA) to assess the relationship between the color
148 traits and the morphology traits, specifically the degree to which variation in multivariate
149 color can be explained by variation in wing morphology. We used permutation ANOVA to

150 assess statistical significance of the model and each RDA axis. We found statistical support
151 for the first RDA axis, which represents a linear combination of morphological traits that
152 predicts the most variation in wing color. We retained this axis for phenotypic selection
153 analysis (18), to assess whether any selection on color remains when accounting for this
154 shared variation with wing morphology.

155 Second, to identify the vector of multivariate color traits most closely associated with
156 fitness, we use projection pursuit regression (29, 30) with the 12 color PCs as predictors and
157 the proportion of offspring sired as the response. We included the total number of offspring
158 from each vial as a weight term. From this analysis we extracted the linear combination of
159 color traits that is the strongest predictor of reproductive success. We then retained this axis,
160 interpretable as the combination of color traits that correlates most strongly with fitness. This
161 approach allowed us to then perform a classical phenotypic selection analysis with only two
162 multivariate traits; multivariate color that appears to be under selection, and the axis of
163 morphological variation that most strongly predicts color.

164 We then performed a phenotypic selection analysis where we fit separate GLMS with
165 binomial (red:brown offspring number) reproductive success as a response and either the
166 projection pursuit axis (color) as a single predictor of fitness, as well as a second model with
167 both this projection persuit axis (color) and the first RDA axis (morphology) as predictors.
168 These two models allow us to assess if there is significant selection on wing interference
169 color that is independent of any selection acting on morphology. We also performed a non-
170 linear phenotypic selection analysis with both predictors in the same model and including
171 quadratic and correlational selection terms. Finally, we repeated our selection analysis using
172 our inferences of wing thickness. We did not include color traits in these selection models as
173 wing thickness was calculated directly from the color data. All selection analyses were
174 performed using absolute fitness, as competition among mates occurred in the vials from

which individual fitness was measured. All traits were mean centered and variance-standardized for fitting regressions. Data and code are available at https://doi.org/10.5281/zenodo.13358353

Results

We obtained complete data on wing color, morphology, and fitness for a total 170 male flies, with fitness data representing eye color score for 7875 total offspring. Wing color traits were generally highly correlated both within and across wing panels (Figure 2). A redundancy analysis (RDA) revealed that 16% of the variation in multivariate wing color can be explained by (is redundant with) the 21 wing size and shape variables (permutation ANOVA $F_{21,148} = 1.34$, $P = 0.0002$). Permutation ANOVA revealed statistical support for the first RDA axis ($F_{1,157} = 5.92$, $P = 0.016$), but not lower axes (all $P \geq 0.097$). Relationships between color traits and wing morphology are illustrated in Figure 2. In a simplified analysis of mean red, green, and blue values across the entire wing, we found similar conclusions (16.7% of mean color variation explained by wing morphology; permutation ANOVA $F_{21,148} = 1.41$, $P = 0.062$). We also found similar conclusions in an RDA predicting wing depth from morphology (17.4% of wing thickness variation explained by wing morphology; permutation ANOVA $F_{21,135} = 1.35$, $P = 0.096$). Our inference of wing thickness indicate wing thickness of approximately 300 nanometers (Figure 3), generally consistent with past work (5, 31) as well as our own observations that wings of LH_m *Drosophila* are just thinner than the usable axial resolution limit of an oil immersion light microscope. There were significant differences among wing panels, with panels 2 and 4 inferred to have greater thickness on average than panels 1 and 3. Depth measures were strongly correlated across wing panels, with positive correlation between panel 1 and 2 depth, 3 and 4 depth, and negative correlations across panels 1,2 and 3,4 (Figure S2).

200 A univariate binomial GLM revealed significant directional selection along the axis of
201 color variation identified through a projection pursuit rotation of the color data (Table 1,
202 Figure 4A). However, including the axis of morphological variation that best predicts wing
203 color (RDA 1) in the GLM revealed this morphological axis as a target of selection; inclusion
204 of RDA 1 led to a 15-fold reduction in inferred strength of directional selection on this axis of
205 multivariate color (Table 1). Consistent with these results, we found that there was a
206 significant phenotypic correlation between the combination of color traits identified by the
207 projection pursuit and the combination of morphological traits that best explains color
208 variation (correlation between PPA 1 and RDA 1, r = -0.31, t_{168} = -4.23 P = 0.000037; Figure
209 S3). Total selection on RDA 1 was a combination of directional and stabilizing (Figure 4B).
210 A full nonlinear selection analysis (32), including both linear terms for color and wing
211 morphology, nonlinear (quadratic) and the interaction (correlational selection) led to similar
212 conclusions and revealed some weak support for correlational selection on wing morphology
213 and color (Table 2). The full response surface is illustrated in Figure 5.
214 The full analysis of directional selection on all 33 traits (Table S1) reveals that
215 significant phenotypic selection on color does remain after accounting for wing size and
216 shape variation, suggesting that while the axis of total selection on color identified in the
217 projection pursuit is primarily apparent, direct selection on other combinations of color traits
218 is direct. Nonetheless, directional selection was by far strongest on univariate centroid size
219 ($|\beta|$ = 0.66; Table S1), itself a measure related to overall body size, with weaker selection
220 acting on multivariate color ($|\boldsymbol{\beta}|$ = 0.65; Table S1) and shape ($|\boldsymbol{\beta}|$ = 0.64; Table S1), noting
221 the vast differences in dimensionality between centroid size (1) and the vectors of selection
222 on color (12) and shape (20). In a selection analysis with all 12 color traits and only a single
223 axis of morphological variance – RDA 1 – we found that the strength of selection was
224 stronger on this single morphological axis ($|\beta|$ = 0.68; Table S2), than on the suite of 12

225 color traits shape (**|$\boldsymbol{\beta}$|** = 0.55; Table S2). Taken together, these results indicate that
226 significant directional selection on wing color remains when accounting for wing size and
227 shape variation, although selection is generally stronger on wing size and shape.
228 We repeated the above selection analysis but focusing on a different, simplified set of
229 measurements of whole-wing mean red, green and blue values from the same individuals.
230 The simplified nature of these color measurements allowed us to include them all in a
231 traditional selection analysis, rather than using projection pursuit to first rotate the data. We
232 found significant directional selection on all three mean color channels, even when including
233 the first RDA axis from a redundancy analysis using these three color variables as a response
234 (Table 3). This analysis revealed evidence for selection on both wing color and wing
235 size/shape acting independently; directional selection was strongest on average red value and
236 wing morphology (Table 3).
237 Finally, in a phenotypic selection analysis focused on wing thickness, we found
238 evidence of significant positive directional selection on wing thickness for wing panels 1 and
239 4, even when accounting for selection on the axis of wing morphology that best predicts color
240 variation (Table 4). Selection on wing thickness was strongest for panel 4 (β = 0.38), nearly
241 as strong as selection on wing shape. Refitting a fully quadratic model for these two traits
242 revealed a fitness surface characterized by direction selection on wing shape (β = -0.5, SE =
243 0.02, $P < 2\text{x}10^{-16}$) and panel 4 thickness (β = 0.28, SE = 0.035, $P < 1.6\text{x}10^{-15}$; Figure 5).
244 Notably, there was significant correlational selection (γ = 0.16, SE = 0.0353 $P < 9.5\text{x}10^{-7}$;
245 Figure 5) in that directional selection for wing thickness was strongest for wings with a low
246 loading on RDA 1, corresponding to wings that are small and non-elongated.
247
248 **Discussion**

249 Using a competitive mating assay combined with morphometric analysis, we have shown that
250 a complex combination of wing interference color and multivariate morphology appear to be
251 targets of phenotypic sexual selection in *Drosophila melanogaster*. While total sexual
252 selection acts on multivariate wing color, the primary axis of total selection on wing color is
253 partly apparent, a result of a small but significant fraction of wing color variation that is
254 explained by variation in wing shape and size: there was strong directional/stabilizing
255 selection on the multivariate combination of wing shape and size that most strongly
256 correlated with color variation. Inclusion of this correlated wing shape/size trait in a
257 phenotypic selection analysis reveals that wing size and shape are the primary targets of
258 selection in our laboratory study, in terms of both statistical significance but also as measured
259 by standardized directional selection gradients. In total, selection was approximately twice as
260 strong on the combination of wing size and shape compared to selection on color. However,
261 selection on color traits does remain after accounting for variation in wing size and shape,
262 suggesting that wing color or thickness may indeed play a role in sexual selection. A major
263 conclusion from our study is that interpreting fitness effects, or evolutionary response, of
264 wing interference colors may be difficult without other measures of wing phenotype,
265 although our results generally support past conclusions (5, 12, 13) that wing interference
266 colors may indeed be a target of sexual selection.

267 Although our approach to measuring reproductive fitness is a relatively standard
268 method in *Drosophila*, it differed from behavioral mating assays of past studies of selection
269 on wing interference. For example, other studies have recorded time to mating in no-choice
270 assays as a measure of reproductive fitness, including manipulation of the background
271 conditions that presumably affect the visibility of wing interference patterns (5, 13). While
272 these past studies did not analyze wing shape variation and its fitness effects in the manner
273 taken here, they did manipulate the selective environment to demonstrate that selection on

these display traits indeed varies with the visual environment, as expected if they are a direct target of selection. This is in contrast to our methods, where we performed an assay of competitive reproductive success by scoring phenotypes of offspring resulting from 24 hours of potential mating, and while we measured traits expected to be correlated with wing color (i.e., performed a multivariate selection analysis; 18, 19), we made no effort to make wing interference patterns visible beyond what is typically observed in a standard fly vial under ambient light. Despite this different approach, we none the less recovered evidence of sexual selection on interference patterns, although we do not find pervasive evidence of stabilizing selection, as observed for wing hue by Katayama et al. (2014).

We found that a small but significant fraction of interference color variation was redundant with wing size and shape. This redundancy was surprisingly low given that wing interference color is a function of wing thickness, which we may expect to be related to wing size and shape (33). One explanation is that wing microstructure (6) such as hair density contributes to wing thickness independently of wing size and shape. Using inverse colorimetry to infer wing thickness from images of interference color, we found some evidence for positive directional selection on wing thickness. This is consistent with the idea that wing color may correlate with quality or condition (34, 35), as has been previously suggested could be the case for *Drosophila* wing interference patterns (5). However, we also found that wing thickness measures correlated in complex ways with each other, suggesting that the relationship between wing thickness and condition may not be straightforward. One explanation could be if wing hair density contributes to interference color, as it likely does (6). Regardless, our analysis of wing thickness should be viewed as preliminary; without a calibrated interferometer or some other independent measure of wing thickness (e.g., 10), our measures of thickness primarily represent a proof of concept. Intriguingly, we found evidence of correlational selection on wing thickness and morphology, in that directional

selection on panel 4 thickness was strongest for smaller wings (see Figure 6), suggesting that selection acts on combinations of wing size, shape, and thickness (color).

We focused on a relatively limited set of color and morphology measures: mean RGB values from four wing panels, as well as 12 morphometric landmarks. Yet even this limited set of raw traits result in a total of 33 total dimensions of color, size, and shape variance, making analysis and interpretation challenging. Our approach was to focus on a set of reduced dimensions of trait variation that focus on the combinations of traits we were specifically interested in, namely the combination of color traits most closely associated with fitness, and the combination of wing size/shape traits most closely associated with color variation. Nonetheless, our qualitative conclusions were largely robust to this approach.

Fly wings provide a case study for the challenges of understanding evolution of phenotypic variation. Although simple in structure, *Drosophila* wings harbor patterns of conserved multivariate variation that has been conserved for millions of years (15). Relatively little is known about the contribution of selection to shaping this and other examples of deeply-conserved variation (36-38), yet it seems likely that coupling measures of multivariate fitness surfaces (39, 40) with estimates of standing variation may be fruitful in illuminating how selection may maintain patterns of multivariate variation. Future work that bridges evolutionary genetics and comparative biology may provide insight into how selective forces acting on complex traits can generate conservation of variation in deep time.

Table 1. Selection analysis of multivariate wing color and morphology. From a binomial GLM with absolute reproductive success (number of red offspring = success, brown = fail) as the response

	color + morphology			**color**		
Predictors	*Estimate*	*std. Error*	*p*	*Estimate*	*std. Error*	*p*
(Intercept)	0.81	0.03	**<0.001**	0.78	0.02	**<0.001**
ppaC	0.01	0.03	0.740	0.15	0.02	**<0.001**
RDA1	-0.51	0.03	**<0.001**			

Table 2. Nonlinear selection analysis of multivariate wing color and morphology. From a binomial GLM with absolute reproductive success (number of red offspring = success, brown = fail) as the response

	binomial mating success		
Predictors	*Estimate*	*std. Error*	*p*
(Intercept)	0.90	0.04	**<0.001**
ppaC	0.01	0.03	0.626
RDA1	-0.49	0.03	**<0.001**
(ppaC)^2	0.04	0.02	**0.030**
(RDA1)^2	-0.12	0.02	**<0.001**
ppaC * RDA1	0.06	0.03	**0.047**

Table 3. Selection on whole wing color data and morphology. From a binomial GLM with absolute reproductive success (number of red offspring = success, brown = fail) as the response

	binomial mating success		
Predictors	*Estimate*	*std. Error*	*p*
(Intercept)	0.79	0.02	**<0.001**
Red mean	0.52	0.06	**<0.001**
Blue mean	0.08	0.03	**0.010**
Green mean	-0.22	0.06	**<0.001**
RDA1	-0.46	0.03	**<0.001**

Table 4. Selection analysis of wing depth and morphology. From a binomial GLM with absolute reproductive success (number of red offspring = success, brown = fail) as the response

	binomial mating success		
Predictors	*Estimate*	*std. Error*	*p*
(Intercept)	0.79	0.03	**<0.001**
d1	0.17	0.06	**0.003**
d2	-0.01	0.04	0.732
d3	-0.01	0.04	0.825
d4	0.38	0.04	**<0.001**
RDA1	-0.58	0.03	**<0.001**

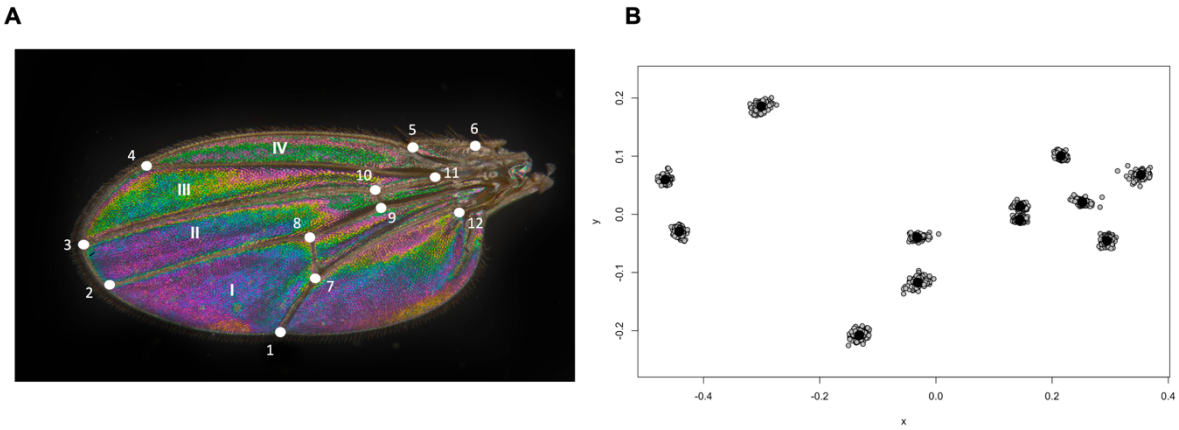

Figure 1. Image analysis of fly wings. Panel **A** shows wing interference color patterns produced under episcopic illumination by optical thin-film interference; wings are transparent when viewed under transmitted light. Also shown in **A** are the 12 landmarks used in analysis of wing shape as well as the four wing panels selected for measurement of rgb color. Panel **B** shows landmark variation after Procrustes rotation and scaling.

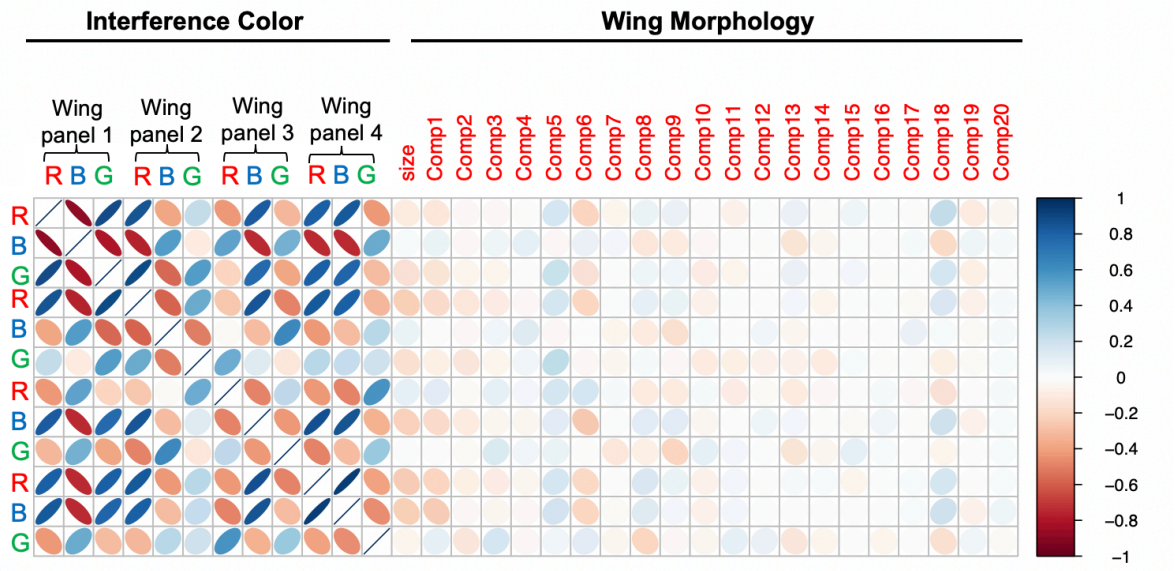

Figure 2. Correlations between wing color and morphology. Shown are the correlations between RGB color values for each wing panel, and the correlation between each of these color traits and the 21 morphological traits from the geometric morphometric analysis. Although correlations between color traits and morphology were far weaker than correlations between color traits, a redundancy analysis revealed a significant (16%) fraction of color variation can be explained by wing size and shape (see text).

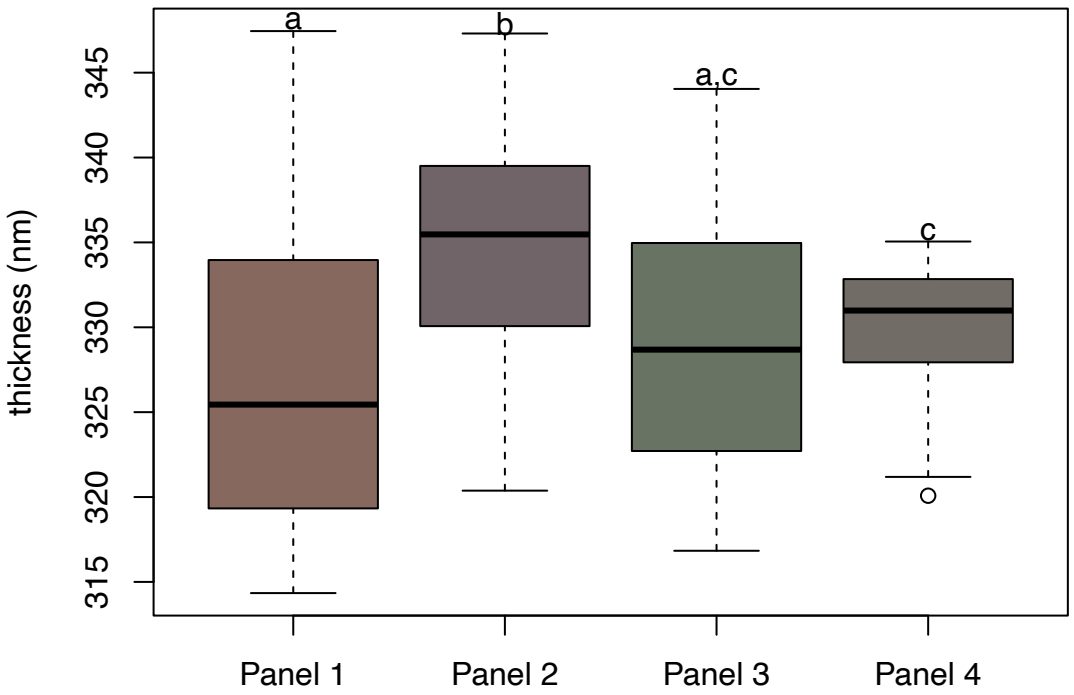

Figure 3. Inferred wing thickness across the four measured wing panels. Each box and whisker plot is colored according to the mean RGB triplet for that panel. Letters denote statistical significance of pairwise contrasts from a multiresponse mixed model. See text for details on inference of thickness.

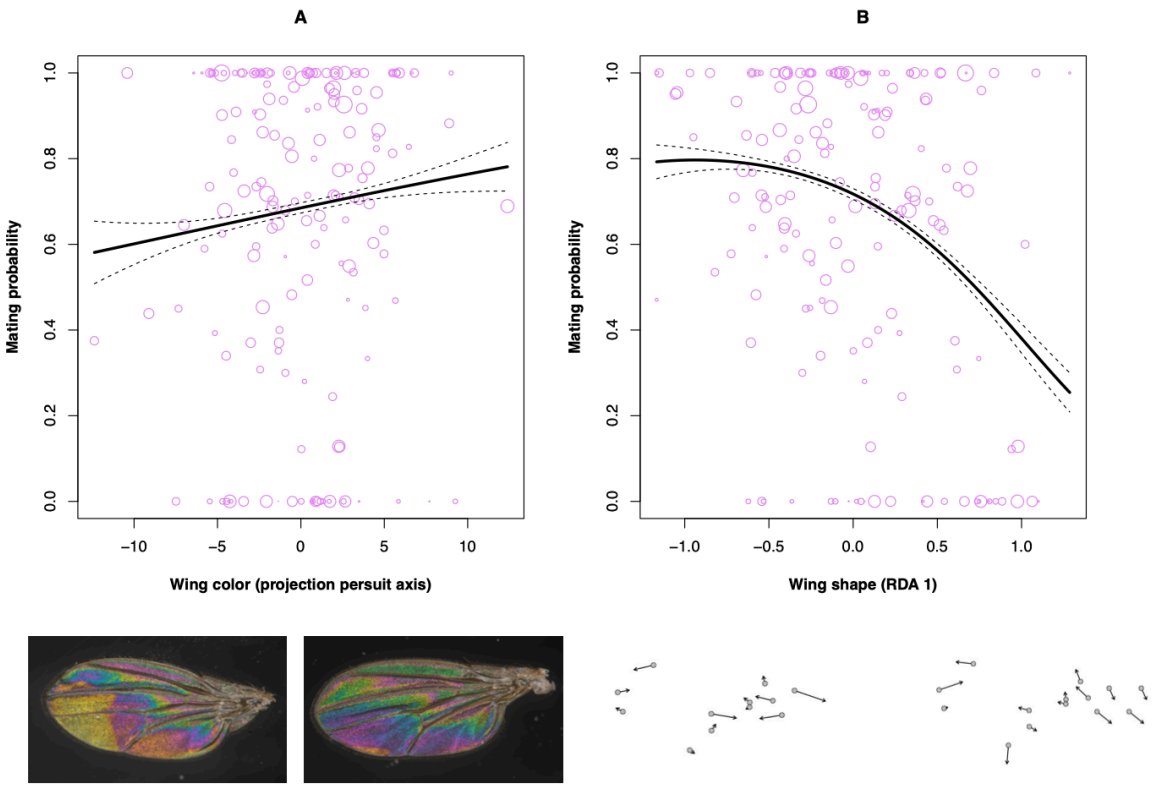

Figure 4. Univariate selection on wing color and morphology. Panel **A** shows the relationship between mating success and multivariate wing color as recovered from a projection pursuit regression of all color traits on mating success; this represents the direction in color space most associated with fitness. Panel **B** shows the relationships between mating success and multivariate wing morphology, in this case the direction of wing shape that most strongly predicts variation in wing color. Images below each panel illustrate the extremes of wing color and wing shape corresponding to each x axis.

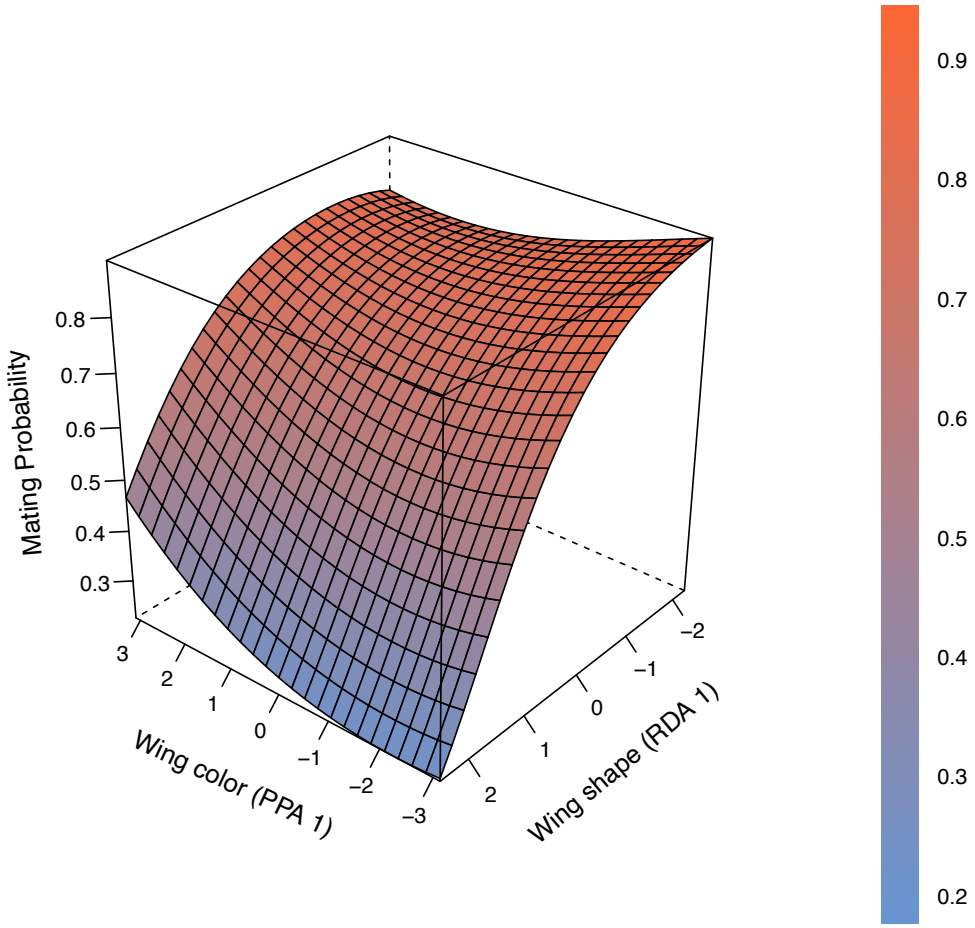

Figure 5. Multivariate selection on wing color and morphology. Shown is response surface from a multiple regression with mating success (binomial) as the response variable and all linear and nonlinear terms for wing color and wing shape. There was no significant directional selection on wing color after accounting for wing shape. See also Table 2.

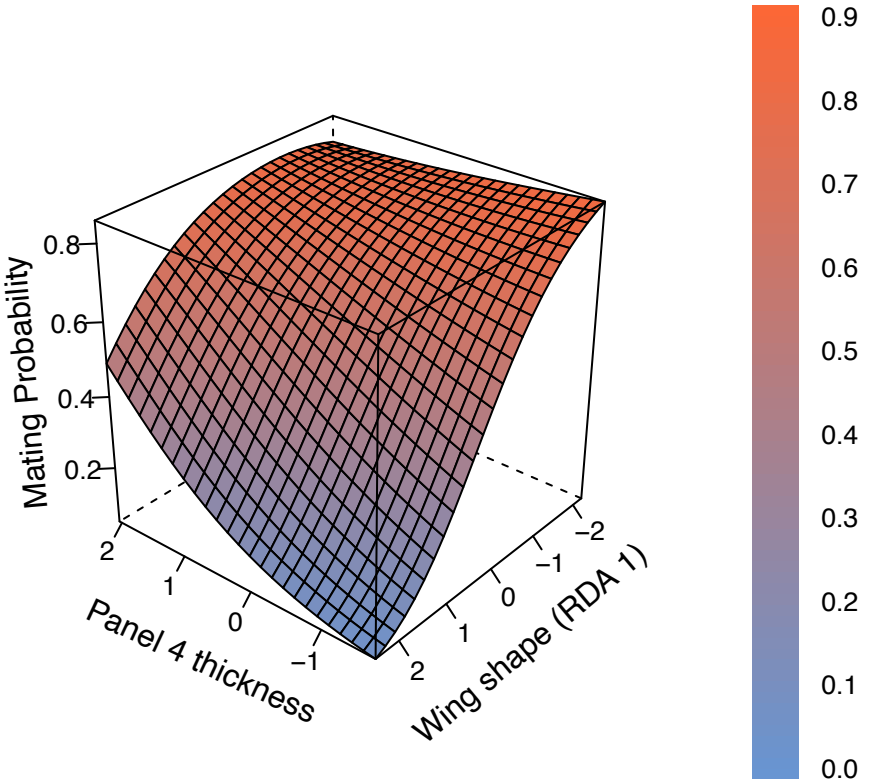

Figure 6. Multivariate selection on wing depth and morphology. Shown is response surface from a multiple regression with mating success (binomial) as the response variable and all linear and nonlinear terms for wing depth (panel 4) and wing shape (RDA 1. Shown is the response surface for Panel 4 and wing shape because a directional selection analysis for all wing panels revealed these two traits where the most important targets of selection (Table 4).

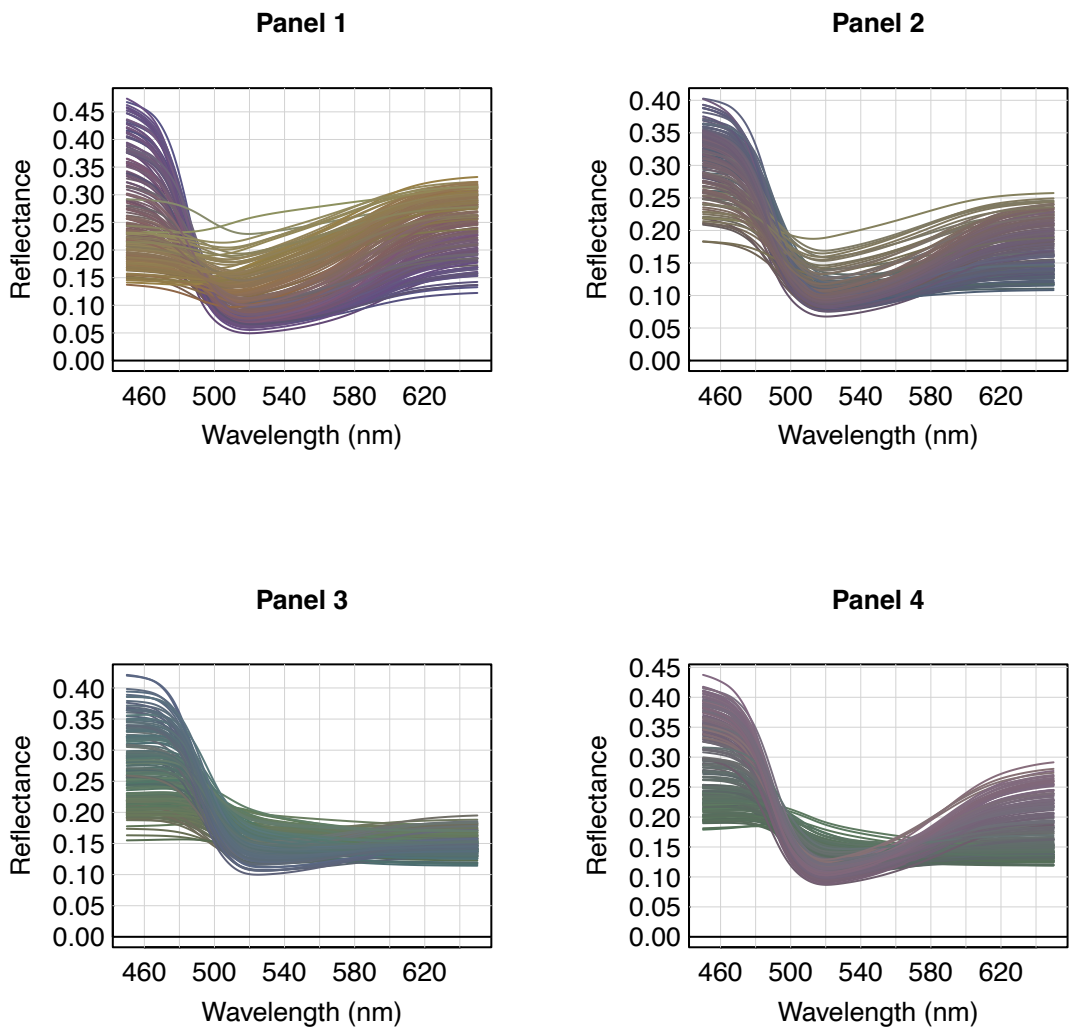

Figure S1. Inferred reflectance spectra for each wing panel. Shown is inferred relationship between the wavelength and reflectance inferred from RGB triplets for each wing panel. Individual curves correspond to individual flies. See text for methodological details.

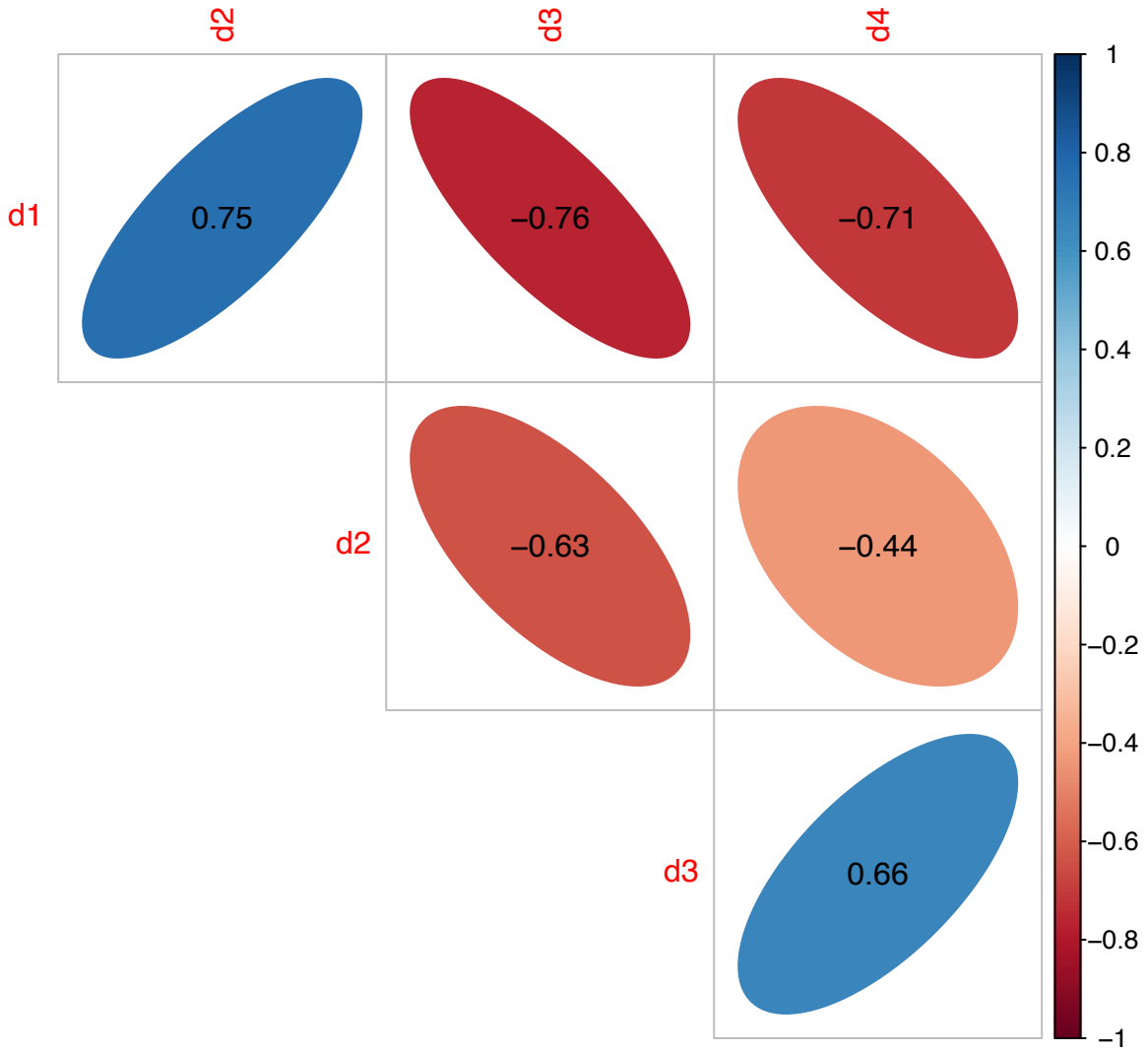

Figure S2. Phenotypic correlation matrix for wing depth. Shown are the phenotypic correlations for inferred wing depth across the four wing panels measured. All correlations were statistically significant.

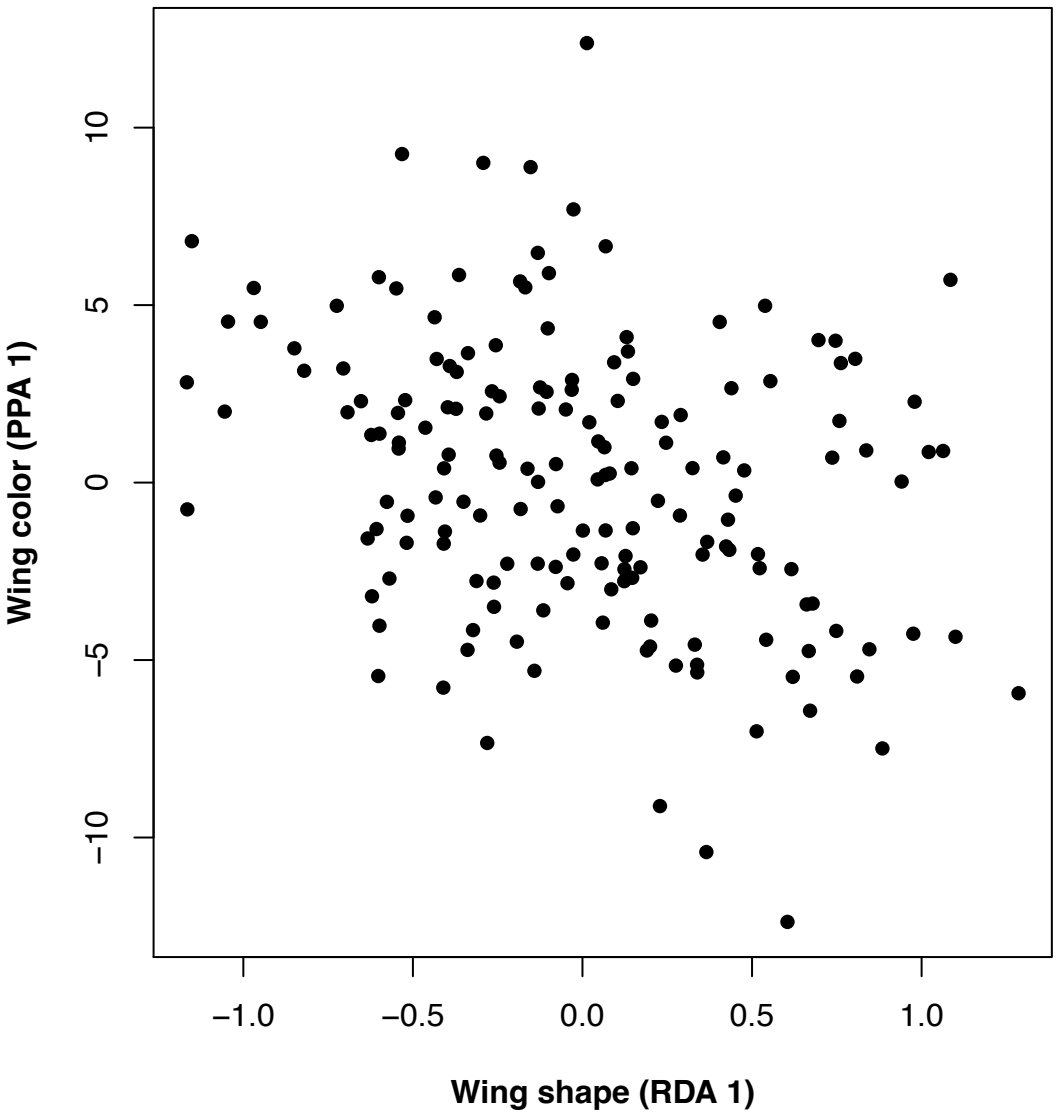

Figure S3. Phenotypic correlation between wing color and wing shape. Shown is relationship between the projection persuit axis of wing color and the first RDA axis of wing morphology.

Table S1. Selection analysis of all color and shape traits

	binomial mating success		
Predictors	*Estimate*	*std. Error*	*p*
(Intercept)	0.88	0.03	**<0.001**
color1	0.34	0.03	**<0.001**
color2	0.05	0.03	0.070
color3	-0.22	0.03	**<0.001**
color4	-0.07	0.03	**0.021**
color5	-0.19	0.03	**<0.001**
color6	0.18	0.03	**<0.001**
color7	0.16	0.03	**<0.001**
color8	0.13	0.03	**<0.001**
color9	-0.11	0.03	**<0.001**
color10	0.11	0.03	**<0.001**
color11	-0.28	0.03	**<0.001**
color12	0.20	0.03	**<0.001**
size	0.66	0.04	**<0.001**
Comp1	0.05	0.03	0.102
Comp2	-0.19	0.04	**<0.001**
Comp3	-0.10	0.03	**0.004**
Comp4	0.13	0.03	**<0.001**
Comp5	-0.31	0.03	**<0.001**
Comp6	0.16	0.03	**<0.001**
Comp7	-0.09	0.03	**0.004**
Comp8	-0.16	0.03	**<0.001**
Comp9	0.06	0.03	**0.038**
Comp10	0.17	0.03	**<0.001**
Comp11	-0.05	0.03	0.077

Comp12	-0.12	0.03	**<0.001**
Comp13	0.14	0.03	**<0.001**
Comp14	0.22	0.03	**<0.001**
Comp15	-0.05	0.03	0.125
Comp16	0.11	0.03	**<0.001**
Comp17	-0.17	0.03	**<0.001**
Comp18	0.00	0.03	0.998
Comp19	0.03	0.03	0.255
Comp20	-0.17	0.03	**<0.001**

Literature Cited

1. Darwin C. The descent of man and selection in relation to sex. London: J. Murray; 1871. 2 v p.
2. Andersson MB. Sexual selection. Princeton, N.J: Princeton University Press; 1994. xx, 599 p. : p.
3. Endler JA. Signals, signal conditions, and the direction of evolution. American Naturalist. 1992;139:S125-S53.
4. Houde AE. Sex, color, and mate choice in guppies. Princeton, N.J: Princeton University Press; 1997. xii, 210 p. : p.
5. Katayama N, Abbott JK, Kjaerandsen J, Takahasji Y, Svensson EI. Sexual selection on wing interference patterns in Drosophila melanogaster. Proceedings of the National Academy of Sciences. 2014;111:15144-8.
6. Shevtsova E, Hansson C, Janzen DH, Kjaerandsen J. Stable structural color patterns displayed on transparent insect wings. Proceedings of the National Academy of Sciences. 2011;108:668-73.
7. Newton I. Opticks: or, a Treatise of the Reflexions, Refractions, Inflexions and Colours of Light. London: Sam. Smith, and Benj. Walford; 1704.
8. Hosseini F, Lotfalizadeh H, Norouzi M, Dadpour M. Wing interference colours in Eurytoma (Hymenoptera: Eurytomidae): variation in patterns among populations and sexes of five species. Systematics and Biodiversity. 2019;17:679–89.
9. Butterworth NJ, White TE, Byrne PG, Wallman JF. Love at first flight: wing interference patterns are species-specific and sexually dimorphic in blowflies (Diptera: Calliphoridae). Journal of Evolutionary Biology. 2021;34:558-70.
10. Li M, Runemark A, Hernandez J, Rota J, Bygebjerg R, Brydegaard M. Discrimination of Hover Fly Species and Sexes by Wing Interference Signals. Advanced Science. 2023;10:2304657.
11. Takahashi KH. Quantitative analysis of wing interference patterns in Drosophila spp. using hyperspectral images. Physiological Entomology. 2022;48:83-9.
12. Hawkes MF, Duffy E, Joag R, Skeats A, Radwan J, Wedell N, et al. Sexual selection drives the evolution of male wing interference patterns. Proceedings B. 2019;286:201828508.
13. Li Q. The colors we didnt see: The Heritability of Wing Interference Pattterns and Their roles in Female Choice in Drosophila melanogaster. Lund: Lund University; 2014.
14. Greenspan RJ, Ferveur JF. Courtship in Drosophila. Annual Reviews Genetics. 2000;34:205-32.
15. Houle D, Bolstad GH, van der Linde K, Hansen TF. Mutation predicts 40 million years of fly wing evolution. Nature. 2017;548:447-50.
16. Houle D, Meyer K. Estimating sampling error of evolutionary statistics based on genetic covariance matrices using maximum likelihood. Journal of Evolutionary Biology. 2015;28:1542-9.
17. Sztepanacz JL, Houle D. Allometry constrains the evolution of sexual dimorphism in Drosophila across 33 million years of divergence. Evolution. 2021;75:1117-31.
18. Lande R, Arnold SJ. The measurement of selection on correlated characters. Evolution. 1983;37(6):1210-26.
19. Svensson EI. Phenotypic selection in natural populations: what have we learned in 40 years? Evolution. 2023;77:1493-504.
20. Arnold SJ, Wade MJ. On the measurement of natural and sexual selection: Applications. Evolution. 1984;38:720-34.

21. Chippindale AK, Gibson JR, Rice WR. Negative genetic correlation for adult fitness between sexes reveals ontogenetic conflict in *Drosophila*. Proceedings of the National Academy of Sciences of the United States of America. 2001;98(4):1671-5.
22. De Lisle SP. Genotype x Environment interaction and the evolution of sexual dimrophism: adult nutritional environment mediates selection and expression of genetic variance in D. melanogaster. Journal of Evolutionary Biology. 2024;in press.
23. De Lisle SP, Svensson EI. On the standardization of fitness and traits in comparative studies of phenotypic selection. Evolution. 2017;71:2313-26.
24. Adams DC, Otárola-Castillo. geomorph: an R package for the collection and analysis of geometric morphometric shape data. Methods in Ecology and Evolution. 2013;4:393-9.
25. Schindelin J, Arganda-Carreras I, Frise E, Kaynig V, Longair M, Pietzsch T, et al. Fiji: an open-source platrform for biological image analysis. Nature Methods. 2012;9:676-82.
26. Stevens M, Párraga CA, Cuthill IC, Partridge JC, Troscianko TS. Using digital photography to study animal coloration. Biological Journal of the Linnean Society. 2007;90:211-37.
27. Davis G. colorSpec: Color Calculations with Emphasis on Spectral Data. R package version 15-0, https://CRANR-projectorg/package=colorSpec. 2024.
28. Davis G. A Centroid for Sections of a Cube in a Function Space, with application to Colorimetry. ArXiv preprints. 2019;1811.00990, https://arxiv.org/abs/1811.00990.
29. Schluter D, Nychka D. Exploring fitness surfaces. American Naturalist. 1994;143:597-616.
30. Morrissey MB. In search of the best methods for multivariate selection analysis. Methods in Ecology and Evolution. 2014;5:1095-109.
31. Hadjaje S, Andrade-Silva I, Dalbe M-J, Clément R, Marthelot J. Wing expansion in Drosophila melanogaster. BioRxiv. 2024;https://doi.org/10.1101/2024.05.17.594352.
32. Phillips PC, Arnold SJ. Visualizing multivariate selection. Evolution. 1989;43:1209-22.
33. Weber KE. Selection on wing allometry in Drosophila melanogaster. Genetics. 1990;126:975-89.
34. Rowe L, Houle D. The lek paradox and the capture of genetic variance by condition dependent traits. Proceedings of the Royal Society of London Series B-Biological Sciences. 1996;263(1375):1415-21.
35. Bonduriansky R. The evolution of condition-dependent sexual dimorphism. The American Naturalist. 2007;169(1):9-19.
36. McGlothlin JW, Kobiela ME, Wright HV, Mahler DL, Kolbe JJ, Loso JB, et al. Adaptive radiation along a deeply conserved genetic line of least resistance in Anolis lizards. Evolution Letters. 2018;2:310-22.
37. De Lisle SP, Bolnick DI, Stuart YE. Predictable and divergent change in the multivariate P matrix during parallel adaptation. The American Naturalist. 2024;204:15-29.
38. Henry GA, Stinchcombe JR. Strong selection is poorly aligned with genetic variation in Ipomoea hederacea: implications for divergence and constraint. Evolution. 2023;77:1712-9.
39. Hohenlohe PA, Arnold SJ. MIPoD: A hypothesis-testing framework for microevolutionary inference from patterns of divergence. American Naturalist. 2008;171(3):366-85.
40. Punzalan D, Rowe L. Concordance between stabilizing sexual selection, intraspecific variation, and interspecific divergence in Phymata. Ecology and Evolution. 2016;6(22):7997-8009.